Available online at www.sciencedirect.com

ScienceDirect

Energy Procedia 78 (2015) 1593 – 1598

Energy Procedia

6th International Building Physics Conference, IBPC 2015

ECCENTRIC Buildings: Evaporative Cooling in Constructed ENvelopes by Transmission and Retention Inside Casings of Buildings

Eric Teitelbaum[a]*, Forrest Meggers[a,b,c], George Scherer[b], Prathap Ramamurthy[b,d], Louis Wang[c], Elie Bou-Zeid[b]

[a]*Princeton University, School of Architecture, Princeton, NJ, 08544, USA*
[b]*Princeton University, Civil and Environmental Engineering, Princeton, NJ, 08544, USA*
[c]*Princeton University, Andlinger Center for Energy and the Environment, Princeton, NJ, 08544, USA*
[d]*The City College of New York, Department of Mechanical Engineering, New York, NY, 10031, USA*

Abstract

New research on evaporative cooling and breathable walls has demonstrated the potential for smart designs where conductive, convective, and radiative heat fluxes are matched or supplemented through low-energy natural phenomena such as wet-bulb temperature depression associated with evaporation. This research seeks to examine the operational and theoretical performance of novel vapor permeable evaporative cooling membrane layers. Latent heat is removed through the evaporation of water through the membrane, where contaminants remain in solution as the hydrophobic membrane allows for passage of only water vapor. Through steady-state analysis of a proposed cooling system for building exterior walls, cooling capacity was shown to exceed cooling loads for large indoor areas. Candidate materials produced from recycled glass were examined through sintering, hydrophobing, and other processes to create materials with the requisite properties specified by simulations. Real data acquired for Princeton, NJ from July 2011 was inputted to the simulations to quantify behavior of the system under real conditions. Even in the humid climate of New Jersey in July, the system can supplement a conventional cooling system, acting as a buffer between interior and external environments. Additionally, the novel mathematical model developed to simulate this evaporative process is in 0.04 ± 0.28 °C agreement to measured data.

Peer-review under responsibility of the CENTRO CONGRESSI INTERNAZIONALE SRL

Keywords: Evaporative Cooling; Passive Cooling; Wet Bulb Depression; Porous Ceramics; Cooling Wall

* Corresponding author. Tel.: +1-609-408-7786; fax: +1-609-258-4740.
E-mail address: eteitelb@princeton.edu

Peer-review under responsibility of the CENTRO CONGRESSI INTERNAZIONALE SRL
doi:10.1016/j.egypro.2015.11.218

1. Background

A building constructed in any environment cannot be entropically isolated from the universe, a fundamental proposition of thermodynamics. As such, energy efficiency must be considered in the larger context of the natural environment, rather than the individual efficiencies of boilers, compressors, etc. [1]. In this sense, the usefulness of the application of an energy source is quantified through exergy analysis. Such an analysis demonstrates the effectiveness of low-temperature heating and high-temperature cooling, which minimize the energy input required by the system because these heating and cooling modes do not require large temperature differentials. Instead, thoughtfully engineered and applied systems can produce heating and cooling with temperatures much closer to the desired temperature.

The focus of this paper is a high-temperature cooling system, namely evaporative cooling through a vapor-permeable membrane, which leverages wet-bulb temperature depression by latent heat removal through evaporation as the cooling mechanism. The advantages are primarily associated with energy savings from spontaneous evaporation, as compared to the energy intensive mechanical vapor-compression cycles and air distribution fans. Additionally, occupant comfort is a function of convective, conductive, and radiant heat transfer, of which the final item rarely receives consideration with respect to cooling among buildings. Evaporative cooling produces a chilled working fluid that can easily be implemented as the temperature source for radiant cooling.

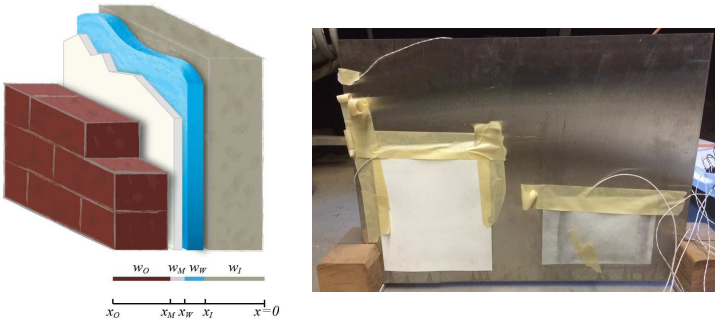

Fig. 1. (a) Proposed evaporative cooling system (b) test structure with a porous, hydrophobic membrane on the left, and nonporous, hydrophilic membrane on the right

The cooling system depicted in Fig 1a operates by maintaining a filled cavity of water (blue) in contact with the building structure (gray) and a vapor permeable membrane (white). A highly porous rain screen (depicted as brick) is employed to protect the membrane. The membrane allows latent cooling to occur through evaporation of water, but restricts the passage of liquid water as well as the uncontrolled wetting of the interior by outdoor rainfall. The bulk temperature of water is lowered toward the wet-bulb temperature of the system, and this temperature depression can be used for either radiant or conductive air cooling. This study proposes and compares two vapor permeable membranes that restrict the flow of water in the liquid phase, with properties that are optimized for water vapor transport. Several materials have been tested which have in common hydrophobic surfaces that increase the pressure head of water sustained behind the membrane. Initially, a porous ceramic tile design was chosen as it offered a rigid shape that could be adapted as a structural element as well. Slip-casting was chosen as the manufacturing method for these tiles, viable for large scale production, but difficult to achieve for small-scale experiments due to the sensitivity of the slip mixture. For laboratory scale experiments, porous polyethylene was chosen as a substitute since it has similar porosities and pore diameters to the ceramic tiles. Additionally, a nonporous, hydrophilic membrane is examined to offer an alternative approach to mass transport. Mercury intrusion porosimetry (MIP) analysis was used to precisely measure porosities and pore diameters for the materials [3].

A fundamental question answered through comparison of mass and heat transport modes is the true location of the evaporative surface in the modeling. The associated computational model is also developed and presented in depth in this paper, offering a novel approach to compute the latent heat, sensible heat, and mass fluxes through the wall sections.

Nomenclature

C	concentration (kg m^{-3})	*Subscripts*	
d	pore diameter (m)	a	starting spatial location
D	diffusivity (m^2 s^{-1})	b	ending spatial location
H	enthalpy (J kg^{-1})	evap	attributed to evaporation
J	heat flux (W m^{-2})	gain	contributing source
J	mass flux (kg m^{-2} s^{-1})	H_2O	water
k	thermal conductivity (W m^{-1} K^{-1})	I	structural layer
M	molar mass (g mol^{-1})	in	input
p	vapor pressure (N m^{-2})	M	membrane layer
P	pressure (atm)	net	overall
Q	heat flux (W m^{-2})	O	external rain screen layer
R	ideal gas constant (J K^{-1} mol^{-1})	sat	saturation conditions
T	temperature (K)	vap	vaporization
w	width (m)	W	water layer
x	position (m)	w	bulk water
γ	evaporative surface properties (s m^{-1})		
ε	porosity		

2. Methods and Materials

The test wall in Fig. 1b is composed of a sheet of stainless steel, a filled cavity of water and a porous (left) and a nonporous (right) membrane. Temperature sensors monitor the bulk water temperature, and surface temperatures of the membrane and stainless steel, opposite the water cavity. The bulk water temperature, once at equilibrium, can be used to determine the mass flux through the membrane. These values, along with air temperature and humidity were used to validate the mathematical model described in section 2.3.

2.1 Membrane Materials

Research commenced with an examination of crushed glass to produce a porous membrane through sintering that could be hydrophobed to prevent the passage of liquid water. This process was fully examined at Princeton University [3]. For simplicity in fabrication and testing, a polyethylene membrane material with pores 2-7 microns in diameter, ε = 0.3, w_M = 3 mm, manufactured by GenPore was also used. Polyethylene exhibits contact angles roughly 90° with water, smaller than ~130° observed with our homemade crushed glass samples after a hydrophobing treatment with trimethylchlorosilane (TMCS). A higher contact angle leads to a greater pressure head that may be maintained behind the membrane, a consideration eliminated with nonporous membranes.

Additional tests were performed to compare the performance of a nonporous hydrophilic membrane. Since the lack of pores eliminates the possibility of the breakthrough pressure being reached, diffusion is not limited by the maximum pore size allowable as a function of the pressure head of water behind the membrane. The hydrophilic material studied is a commercially produced membrane (Arkema Pebax, w_M < 29μm) designed to facilitate the passage of water vapor by diffusion of liquid water molecules through the hydrophilic membrane structure and evaporation into unsaturated air on the outside.

2.2 Mathematical Model for Quasi-Steady State Mass Transport

At the heart of this analysis is a steady state model that calculates the net heat removal from the building interior as a function of ambient environmental conditions including pressure, temperature, and solar radiation. The net heat flux from the building is the sum all heat fluxes through the wall cross section depicted in Fig. 1a. As such, there is radiative heat gain from solar radiation at the exterior surface Q_{gain}, sensible heat transfer from the building interior

to the water Q_{in}, and the latent heat of evaporation Q_{evap}, all of which must be accounted.

$$Q_{net} = Q_{gain} + Q_{in} - Q_{evap} \tag{1}$$

For this to be true, Q_{evap} must be in psychometric equilibrium with the temperature profile established within the system, which in turn is dictated by solar radiation, atmospheric weather conditions, and the interior building thermostat setpoint. Therefore, solving for the sensible heat removal of the system is not trivial.

$$J_{a,b} = -k_{ab}\frac{T_b - T_a}{w_{ab}} \tag{2}$$

To solve for the net heat flux, J, Eq. 2 must be computed for all parts of the system where k is thermal conductivity, T is temperature, and w is width. Fig. 1a represents the 1D heat transfer through the building structure to the exterior environment. At point $x = 0$, the building structure, i.e. concrete slab, starts and continues to $x = x_1$.

In addition to sensible heat transfer, latent heat removal is responsible for the cooling component of the proposed system. As such, the amount of latent heat removed depends on the amount of water that can leave the system through evaporation. For the case of vapor transport through a microporous membrane, the diffusion mechanism depends on the physical structure of the membrane, as reflected in the Knudsen number, which is the ratio of the mean free path of water vapor diffusing in air and the pore diameter. For large Knudsen numbers, $Kn >> 1$, the mean free path of a water molecule is large relative to the pore diameter, implying that diffusion is restricted by collisions with the pore walls. The same is true for low-pressure systems (large mean free path). For the membrane proposed in this work, $Kn \sim O(0.01 - 1)$, which is in the range where resistance is encountered mainly due to pore geometry; nevertheless, continuum diffusion is still significant. Under these circumstances, the diffusivity of the vapor through the porous membrane, D', with M, the molar mass, and P, atmospheric pressure, is [4]

$$\frac{1}{D'} = \frac{1}{97\left(\frac{d}{2}\right)\sqrt{\frac{T}{M_{H_2O}}}} + \frac{1}{1.87\times10^{-10}\left(\frac{T^{2.072}}{P}\right)} \tag{3}$$

Since diffusion through porous media may only occur through pores that occupy a fraction ε of the volume, a correction of D' must be made to account for the porosity ε. Another correction is required because the tortuous pores increase the path length by a factor of $\tau > 1$. Scanning electron microscopy confirms that the pores are tortuous; approximating the tortuosity as $\tau \approx 1/\varepsilon$, the effective diffusivity is [5].

$$D = \varepsilon D' / \tau \approx \varepsilon^2 D' \tag{4}$$

As with heat conduction, the latent heat transfer due to evaporation is driven by a concentration differential, in this case the difference in saturation vapor pressure of water at the membrane/water interface, and the ambient water vapor pressure of the environment. The mass flux associated with evaporation can be written as

$$J_{evap} = \gamma_{evap}\left(p_{sat}[T_w] - p_M\right) \tag{5}$$

where γ_{evap} typically depends on factors such as wind velocity (when calculating wind chill temperatures) and surface roughness. However, in this system the evaporative surface is not exposed to ambient conditions; therefore γ_{evap} can be assumed to depend solely on temperature. Here, p is vapor pressure of water.

At any given point in the system, the mass flux of water vapor at steady state is given by Fick's law,

$$J = -D\frac{dC_w}{dx} \tag{6}$$

which can be expanded using the ideal gas law to obtain

$$J_M = -\frac{D_M}{R}\frac{d(p/T)}{dx} = -\frac{D_M}{R}\left(\frac{p_M/T_M - p_{sat}[T_W]/T_W}{w_M}\right) \tag{7}$$

One may assume that T_M and T_W are the same since the membrane is thin compared to the system. Since the evaporative flux must equal the mass flux, one can set Eq. 7 equal to Eq. 5:

$$\gamma_{evap}\left(p_{sat}[T_W] - p_M\right) = \frac{D_M}{RT_W}\left(\frac{p_{sat}[T_W] - p_M}{w_M}\right) \tag{8}$$

Through some algebraic manipulations [3], one arrives at the governing equation for the system as follows

$$\frac{p_{sat}[T_W]}{T_W} + T_W\left(\frac{k_I}{w_I} + \frac{k_O}{w_O}\right)\left(\frac{w_M}{D_M} + \frac{w_O}{D_O}\right)\left(\frac{R}{|\Delta H_{vap}|}\right) = \frac{p_O}{T_O} + \left(\frac{k_I T_I}{w_I} + \frac{k_O T_O}{w_O}\right)\left(\frac{w_M}{D_M} + \frac{w_O}{D_O}\right)\left(\frac{R}{|\Delta H_{vap}|}\right) \quad (9)$$

which allows for T_W to be obtained numerically, since $p_{sat}[T_W]$ is an exponential function of temperature. A numeric solver was used in conjunction with an Urban Heat Model developed at Princeton University, which was used to generate surface temperatures of surfaces, i.e. to represent the radiative and convective heat fluxes at the exterior boundary [6]. This model accounts for convective and shortwave and longwave radiative exchanges at the exterior surface; to compute the exterior temperature it also need to estimate wall conduction for which it utilizes a multi-layer Green's function analytical solution in the wall [6]. Based on real atmospheric data from Princeton University in July 2011, values for T_W were chosen initially as 21 °C and plugged into the Urban Heat Model which generated a surface temperature. This surface temperature was then inputted to the membrane model. This iterative approach was repeated until the two models produced values with a 10^{-2} tolerance for successive values of T_W.

3. Experimental Setup

To test the precision and applicability of the model, a test apparatus was developed. The device pictured in Fig. 1b seals a layer of water on average 5 mm thick between a porous membrane and a thin sheet of stainless steel. The setup was outfitted with surface temperature sensors to track the surface temperature of the steel and membrane, and additionally the bulk water temperature was recorded. Sensors logged automatically every minute.

Surface temperature sensors were mounted to both the metal surface opposite contact with water and the membrane surface, also opposite contact with water, to establish the temperature profile within the metal and the membrane. The bulk temperature of the water was assumed to be the temperature boundary condition at the metal/water interface and the membrane/water interface.

These values were recorded and then inputted to a Matlab workspace where simulations were performed to compare the measured bulk water temperature with the theoretically calculated bulk water temperature. These values were used to calculate the cooling capacity per unit area of the system. Given the steady-state temperature from Eq. 9, the heat flux and mass flux through the membrane can be calculated since all surface temperatures for the system are known. The overall heat energy balance is simply

$$\Delta H_{vap}\left(\mathrm{J}_I - \mathrm{J}_O\right) = k_I \frac{T_I - T_W}{w_I} + k_O \frac{T_O - T_W}{w_O} \quad (10)$$

4. Results

Infrared thermal images of the evaporative surface were taken to observe the behavior of the system. Fig. 2a shows both the porous polyethylene membrane and nonporous polypropylene-backed membrane side-by-side in the infrared spectrum. The darker blue for the polypropylene-backed membrane is indicative of a lower surface temperature. This is likely the result of the evaporative surface being on the outside for the nonporous material, and inside at the membrane/water interface for the porous material. The surface temperature difference of 1.3 ± 0.20 °C is larger than the 0.44 ± 0.15 °C average bulk temperature difference between the two systems, confirming the evaporative surface difference.

The full data set is shown in Fig. 2c, comparing both membranes. The red data, for the polypropylene membrane's bulk water temperature is always closer to the wet-bulb temperature than the polyethylene membrane's bulk water temperature. As the wet-bulb temperature is the theoretical boundary for heat and mass transfer equilibrium temperature, a value closer to the wet-bulb temperature corresponds to more mass transfer. Additionally, the restriction on evaporation imposed by both membranes is significant enough that a small decrease in relative humidity, as evidenced by the decreasing trend of the wet-bulb temperature shown in Fig. 2c, does not induce a change in bulk water temperature as it would if the system had a free surface for evaporation. The oscillations in the data are due to the building heating system turning on and off, but this does not have a significant impact on performance because the scale of the system is small enough to minimize thermal lag.

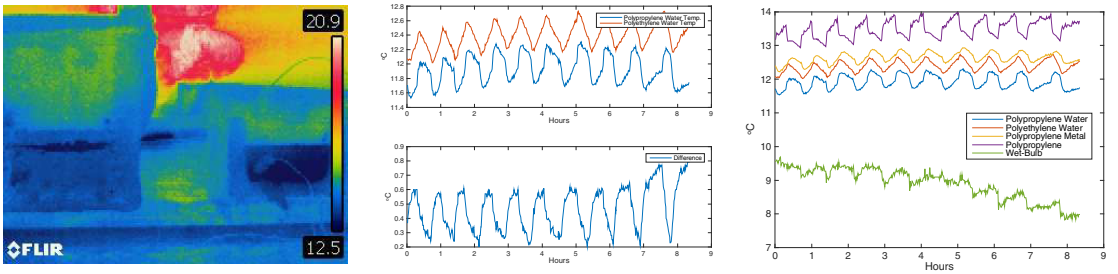

Fig. 2 (a) Porous polyethylene membrane (left side) compared to nonporous polypropylene membrane (right); (b) Real-time comparison of both membranes; (c) Entire data set for both membranes

Fig. 3a shows the full comparison between the theoretical model developed for the system and real observations. For this, the porous polyethylene membrane was used. There is good agreement, with an average of 0.04 ± 0.28 °C difference between the two values. Also shown in Fig. 3b is the predicted heat removal capabilities of the system, shown on the top-right, given the air and water conditions shown on the bottom-right.

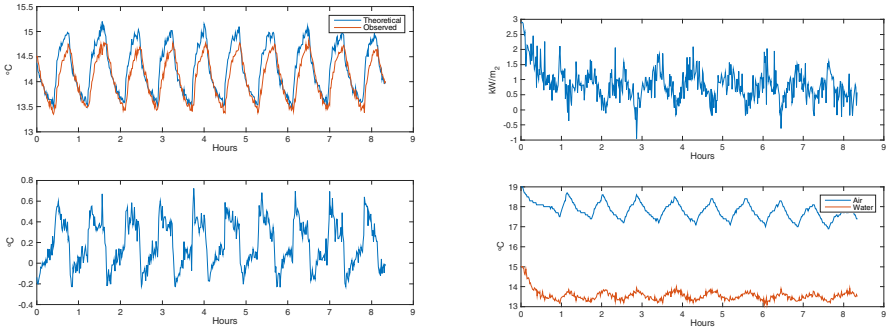

Fig. 3. (a) Theoretical versus observed performance (top) and difference between theoretical and observed performance (bottom); (b) Predicted cooling capacity of system

5. Conclusions and Future Work

The high fidelity between the theoretical model and experimental data from the laboratory confirm the accuracy of the heat and mass transfer model for the phenomena occurring within the system. The hydrophilic membrane material maintained a higher mass flow rate than the porous polyethylene membrane. Future studies could investigate high porosity materials ($\varepsilon > 0.5$) as this would increase overall diffusion through porous media.

References

[1] Moe K. Insulating modernism: Isolated and non-isolated thermodynamics in architecture. Basel, Switzerland: Bierhäuser; 2014.
[2] Smith ST, Hanby VI, Harpham C. A probabilistic analysis of the future potential of evaporative cooling systems in a temperate climate. Energy and Buildings 2011;43:507-516.
[3] Teitelbaum E. Evaporative cooling on building surfaces through a microporous hydrophobic membrane. Undergraduate thesis, Princeton University: Princeton NJ; 2014.
[4] Traum MJ. Latent heat fluxes through nano-engineered porous materials. Ph.D. thesis, Massachusetts Institute of Technology: Cambridge MA; 2007.
[5] Welty JR, Wicks CE, Wilson RE, Rorrer, GL. Fundamentals of Momentum, Heat, and Mass Transfer. Danvers, Massachusetts, USA: John Wiley and Sons, Inc.; 2008.
[6] Wang Z, Bou-Zeid E, Smith JA. A spatially-analytical scheme for surface temperatures and conductive heat fluxes in urban canopy models. Boundary-Layer Meteorology 2011;138:171-193.